UNIVERSITY OF BIRMINGHAM

University of Birmingham Research at Birmingham

Poly lactic-co-glycolic acid controlled delivery of disulfiram to target liver cancer stem-like cells

Wang, Zhipeng; Tan, Jiao; Mcconville, Christopher; Kannappan, Vinodh; Tawari, Patricia Erebi; Brown, James; Ding, Jin; Armesilla, Angel L.; Irache, Juan M.; Mei, Qi-bing; Tan, Yuhuan; Liu, Ying; Jiang, Wenguo; Bian, Xiuwu; Wang, Weiguang

Document Version
Publisher's PDF, also known as Version of record

Link to publication on Research at Birmingham portal

Original Article

nanomedjournal.com

Poly lactic-co-glycolic acid controlled delivery of disulfiram to target liver cancer stem-like cells

Zhipeng Wang, PhD, MD[a], Jiao Tan, MSc[b], Christopher McConville, PhD[c],
Vinodh Kannappan, PhD[a], Patricia Erebi Tawari, PhD[a], James Brown, PhD[d],
Jin Ding, PhD, MD[e], Angel L. Armesilla, PhD[a], Juan M. Irache, PhD[f], Qi-Bing Mei, PhD, MD[g],
Yuhuan Tan, MSc[b], Ying Liu, MSc[b], Wenguo Jiang, PhD, MD[h], Xiu-Wu Bian, PhD, MD[b,i,j,*],
Weiguang Wang, PhD, MD[a,*]

[a]Faculty of Science & Engineering, University of Wolverhampton, Wolverhampton, UK
[b]Institute of Pathology and Southwest Cancer Center, Southwest Hospital, Third Military Medical University, China
[c]School of Pharmacy, University of Birmingham, UK
[d]School of Life and Health Sciences and ARCHA, Aston University, UK
[e]Eastern Hepatobiliary Surgery Hospital, Shanghai, China
[f]School of Pharmacy, University of Navarra, Pamplona, Spain
[g]School of Pharmacy, Fourth Military Medical University, China
[h]Cardiff China Medical Research Collaborative, Cardiff University School of Medicine, Cardiff, UK
[i]Key Laboratory of Tumor Immunopathology, Ministry of Education of China, Chongqing, China
[j]Collaborative Innovation Center for Cancer Medicine, Sun Yat-Sen University, Guangzhou, China

Abstract

Disulfiram (DS), an anti-alcoholism drug, shows very strong cytotoxicity in many cancer types. However its clinical application in cancer treatment is limited by the very short half-life in the bloodstream. In this study, we developed a poly lactic-co-glycolic acid (PLGA)-encapsulated DS protecting DS from the degradation in the bloodstream. The newly developed DS-PLGA was characterized. The DS-PLGA has very satisfactory encapsulation efficiency, drug-loading content and controlled release rate *in vitro*. PLGA encapsulation extended the half-life of DS from shorter than 2 minutes to 7 hours in serum. In combination with copper, DS-PLGA significantly inhibited the liver cancer stem cell population. CI-isobologram showed a remarkable synergistic cytotoxicity between DS-PLGA and 5-FU or sorafenib. It also demonstrated very promising anticancer efficacy and antimetastatic effect in liver cancer mouse model. Both DS and PLGA are FDA approved products for clinical application. Our study may lead to repositioning of DS into liver cancer treatment.
© 2016 The Authors. Published by Elsevier Inc. This is an open access article under the CC BY-NC-ND license (http://creativecommons.org/licenses/by-nc-nd/4.0/).

Key words: Disulfiram; PLGA; Liver cancer; Cancer stem cells; Drug repositioning; Nano-technology; Drug delivery

Primary liver cancer is the fifth most common neoplasm and the third most common cause of cancer-related death worldwide.[1] Hepatocellular carcinoma (HCC) accounts for 70%-80% of cases of primary liver cancer.[2] The incidence of HCC is high in Asia and increasing in the Western world in the past decade. Although the therapeutic outcomes in many cancers have been improved significantly, the prognosis of advanced HCC remains very dismal.[3] Chemoresistance and metastasis are the major hindrances for the treatment of advanced HCC. HCC cells are resistant to all currently available anticancer drugs. Sorafenib (Nexavar) is the sole drug showing marginal efficacy in HCC with only approximately 3 month improvement for overall survival.[4] Therefore, development of efficacious chemotherapeutic drugs is of significant clinical importance for treatment of the advanced HCC.
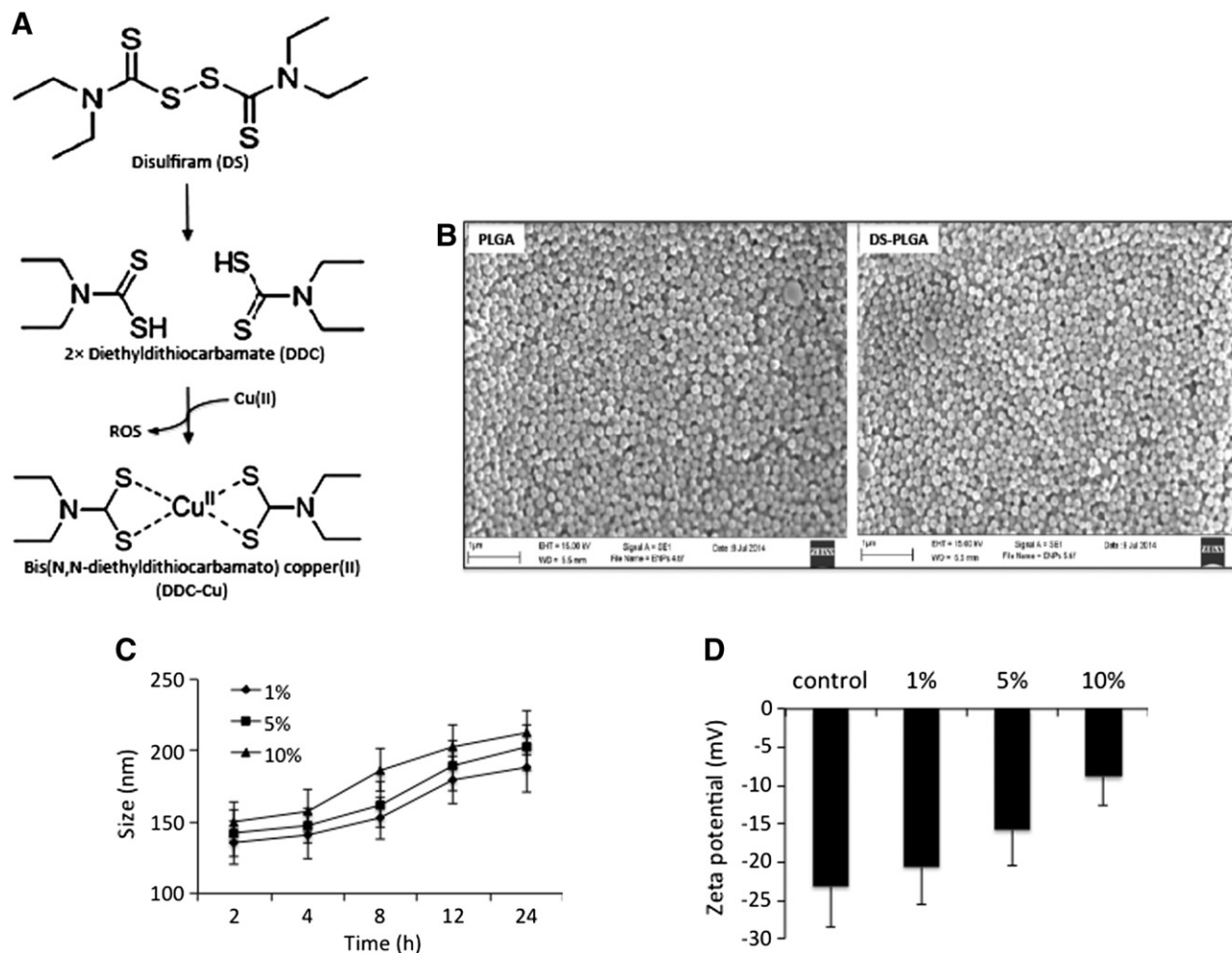
Figure 1. *In vitro* characterization of DS-PLGA. **(A)** The scheme of DS metabolism and reaction with copper(II). **(B)** Scanning electron micrographs of PLGA and DS-encapsulated PLGA (DS-PLGA). **(C)** The influence of serum concentration on the size of DS-PLGA. **(D)** The influence of serum concentration on zeta potential. **(E)** *In vitro* release profiles of DS. **(F)** *In vitro* half-life of DS in horse serum. **(G)** The *in vitro* half-life of free DS and DS-PLGA in horse serum. **$P < 0.01$.

HCC is a highly heterogenic disease containing a small population of cancer stem-like cells (CSCs). HCC CSCs can be identified by detection of the expression of stem cell markers *e.g.* ALDH, CD133, CD90, CD44, EpCAM, and CD13.[5] Previous studies suggest that CSCs are maintained by the hypoxic milieu,[6,7] quiescent and highly resistant to currently available chemotherapeutic agents. Conventional anticancer drugs eliminate bulk of cancer cells but could not eradicate CSCs, which become the source of the cancer recurrence and metastasis. Therefore, development of efficacious CSC-targeting drugs may improve the therapeutic outcomes of HCC.

New drug development is a time and cash consuming procedure. This leads to the current interest in drug repositioning.[8] Previous studies demonstrate that disulfiram (DS), a commercially available anti-alcoholism drug,[9] is highly cytotoxic to a wide range of cancer cell lines[10–13] and enhances conventional anticancer drug-induced apoptosis in colon, breast and brain cancer cell lines.[10,14–16] Importantly, DS is highly cancer specific and specifically inhibits the activity of aldehyde dehydrogenase (ALDH), a functional marker of CSCs and reactive oxygen species (ROS) scavenger[17,18] to eliminate CSCs.

Although the anticancer activity of DS has been reported for almost 3 decades, its translation into clinical cancer treatment is severely limited by its very short half-life in the bloodstream.[19] The anticancer activity of DS is copper (Cu), zinc and some other divalent transitional metal elements dependent.[11,20–22] DS is quickly reduced to diethyldithiocarbamate (DDC), a strong chelator of copper(II). The reaction between DDC and Cu(II) generates ROS which are highly toxic to cancer cells. Due to the extremely short lifespan of ROS in human tissues,[23] the extracellular ROS can target cancer cells only when the reaction takes place within the cancer tissues.[22,24] DDC-Cu, the final product of the DS and Cu reaction, can also penetrate into cancer cells and induce apoptosis.[22] The sulfhydryl group of DDC is essential (Figure 1, *A*) for chelation of Cu(II) by DDC. The currently available oral version of DS is quickly reduced to DDC and the sulfhydryl group of DDC is promptly destroyed by glucuronidation, methylation and degradation in the bloodstream of the portal vein.[25] This may introduce the discrepancy between the anticancer activity of DS *in vitro, in vivo* and in patients. In order to translate DS into cancer therapeutics, intact sulfhydryl group of DS or DDC must be protected in the bloodstream and
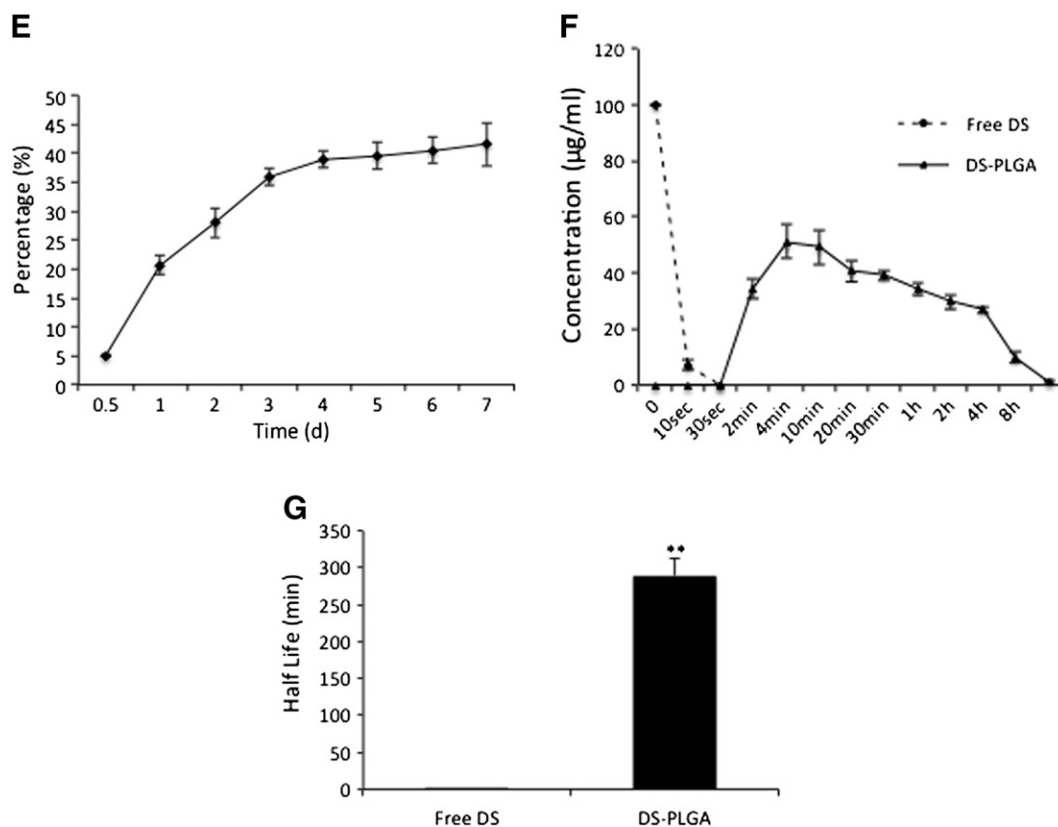
Figure 1 *(continued)*.

delivered to cancer tissues where it reacts with Cu to generate ROS and form DDC-Cu (Figure 1, *A*). We previously showed that encapsulation of DS into liposome extends the half-life of DS and improves its *in vivo* anticancer efficacy in breast cancer mouse model.[6]

The purpose of this study is to develop a long circulating poly lactic-co-glycolic acid (PLGA) encapsulated DS (DS-PLGA) to achieve longer circulating time and improve the anticancer efficacy of DS.

Methods

Materials

The HCC cell lines Huh7 and PLC/PRF/5 were purchased from ATCC (Middlesex, UK). DS, 5-fluorouracil (5-FU), copper chloride (CuCl$_2$), copper gluconate (CuGlu), poly lactic-co-glycolic acid (PLGA), poly(vinyl acetate), cyano-methyl diphenylcarbamodithioate (PVA), dichloromethane, poly-2-hydroxyethyl methacrylate (poly-HEMA) and bovine serum albumin (BSA) were purchased from Sigma (Dorset, UK). DMEM and fetal calf serum (FCS) were supplied by Lonza (Wokingham, UK). Ki-67 and BAX antibodies were purchased from Cell Signaling (Danvers, MA, USA). NFkBp65 and ALDH1 antibodies were from Abcam. Sorafenib was from BioVision (CA, USA). Cell culture inserts were purchased from Fisher (Loughborough, UK). Lipo-DS was provided by Prof. Xing Tang (Shenyang Pharmaceutical University, China).

Preparation and characterization of DS-PLGA nanoparticles

The DS loaded nanoparticles were prepared using an emulsion–solvent evaporation method. PLGA (200 mg) and DS (20, 40, 50, 100 or 150 mg) were dissolved in 10 mL of dichloromethane, and then mixed with 20 mL of 2.5% PVA aqueous solution. This mixture was homogenized for 1 min by vortex and then sonicated using a microtip probe sonicator set at 70% power output (XL 2002 Sonicator® ultrasonic liquid processor) for 3, 4 or 5 min to produce the oil-in-water emulsion. The organic phase was evaporated for 5 h at room temperature. The nanoparticles were recovered by centrifugation (10,000 rpm, 20 min, Hitachi). The nanoparticles were washed twice with water. The purified nanoparticles were freeze-dried in 5% sucrose.

The size distribution and zeta potential of DS-PLGA were measured by DLS using a Zetasizer (ZS90, Malvern, U.K.) with a scatter angle of 90° at 25 °C. The morphology of nanoparticles was observed by scanning electron microscopy (SEM) (JEOL JSM T330A). A drop of the nanoparticle suspension was placed on a metallic surface. After drying under vacuum, the sample was coated with a gold layer.

Measurement of encapsulation efficiency, drug loading content, cumulative release and the in vitro half-life of DS-PLGA

The amount of non-entrapped DS was determined using HPLC by UV detection set at 275 nm (SHIMADZU LC-20). The mobile phase was a mixture of methanol:water (70:30%)

Table 1
Physicochemical parameters of PLGA and DS loaded PLGA nanoparticles.

Nanoparticles	Drug loading content (%)	Encapsulation efficiency (%)	Size (nm)	Zeta potential (mV)
Empty PLGA	–	–	131.8 ± 6.9	22.3 ± 0.8
DS-PLGA	27.67 ± 3.47	78.92 ± 2.16	136.2 ± 6.2	21.7 ± 0.96

and the flow rate was set at 1 ml/min. Separation was achieved using a Phenomenex C18 column (250 mm × 4.6 mm, 5 μm). The amount of DS entrapped in the nanoparticles was determined after their dissolution in dichloromethane. After evaporation of dichloromethane at room temperature, DS was dissolved in pure ethanol. The supernatants were passed through a membrane filter (pore size 0.22 μm, Millipore) before HPLC measurements. The cumulative release profile of DS-PLGA was measured in 0.1 M phosphate buffer solution (PBS, pH 7.4) with 0.5% Tween 80 at 37 °C. In brief, 10 mg DS-PLGA was suspended in 25 ml PBS-Tween80 solution with continuously shaking (100 rpm min^{-1}) at 37 °C. At indicated time intervals, 500 μl of the release media was collected and centrifuged at 14,000 rpm for 10 min at room temperature to remove the PLGA nanoparticles with unreleased DS. The DS concentrations in the supernatant were measured using HPLC and equal volume of fresh media was replenished. The drug loading content (DLC) and encapsulation efficiency (EE) of DS in the PLGA nanoparticles were calculated using the following equations.

$$DLC \ (\%) = Weight \ of \ DS \ in \ PLGA / Weight \ of \ the \ whole \ DS\text{-}PLGA \times 100\%$$

$$EE \ (\%) = (Weight \ of \ total \ DS - Weight \ of \ free \ DS) / Weight \ of \ total \ DS \times 100\%$$

To examine the half-life of DS *in vitro*, free DS or DS-PLGA (100 μl at a concentration of 3 mg/ml) was added into an Eppendorf tube containing 300 μl of horse serum with shaking at 37 °C. The Eppendorf tubes were collected and protein precipitated by adding 300 μl of absolute methanol at different time intervals. The PLGA nanoparticles with unreleased DS were removed by centrifugation at 14,000 rpm for 10 min at room temperature. The DS in the supernatant was determined by HPLC measurement.

In vitro cytotoxicity of DS-PLGA to HCC cells

The PLC/PRF/5 and Huh7 HCC cell lines were cultured in DMEM supplemented with 10% FCS, 50 units/ml penicillin, and 50 μg/ml streptomycin. For *in vitro* cytotoxicity assay, the overnight cultured cells (5000/well) in 96-well flat-bottomed microtiter plates were exposed to drugs for 72 h in normoxic or hypoxic condition and subjected to a standard MTT assay.[16]

Analysis of the combinational effect of 5-FU + DS-PLGA/Cu and sorafenib + DS-PLGA/Cu

The HCC cells were cultured at 5000 cells/well in 96-well plates overnight and then exposed to various concentrations of 5-FU, sorafenib, DS-PLGA/Cu$_{1μM}$, 5-FU or sorafenib in combination with DS-PLGA/Cu$_{1μM}$ at a constant ratio of 5-FU:DS-PLGA and sorafenib:DS-PLGA of 1000:1 and 100:1

respectively. The cells were exposed to different drug combinations for 72 hours subjected to MTT analysis.[16] The IC$_{50s}$ from one and two-drug-treated cells were determined. The combinational cytotoxicity was analyzed by CI-isobologram program using CalcuSyn software (Biosoft, Cambridge, UK).[26] The combination index (CI) was determined by mutually exclusive equations.

Flow cytometric detection of ALDH activity and CD133 expression

The ALDH positive population was detected by ALDEFLUOR kit (StemCell Tech., Durham, NC, USA) following the supplier's instruction. The cells (2.5×10^5) were analyzed after stained in ALDH substrate containing assay buffer for 30 min at 37 °C. Diethylaminobenzaldehyde (DEAB), a specific ALDH inhibitor, treated cells were used as a positive control.

To detect the expression of CD133 positive cells, the cells (2.5×10^5) were incubated with CD133 antibody (BD Pharmingen, Oxford, UK) for 30 min at 4 °C. Unbound antibodies were washed off with 2% FCS HBSS (Sigma). After staining for no longer than 1 h, the positively stained population (10,000 events) was detected using a BD Accuri™ C6 flow cytometer (Becton Dickinson, Franklin Lakes, NJ, USA) with 488-nm blue laser and standard FITC 530/30 nm bandpass filter.

Flow cytometric detection of apoptosis

DNA content was used to detect the apoptotic cells. Briefly, cells (1×10^6) were exposed to drugs and harvested by trypsinization. The cells were fixed in 70% ethanol and then incubated with RNase A (100 μg/ml) and propidium iodide (2.5 mg/ml) for 30 min. The DNA content data from 10,000 cells in each sample was collected by a BD Accuri™ C6 flow cytometer and analyzed using a CellQuest software (BD Biosciences, Oxford, UK).

Clonogenic assay

The overnight cultured cells (5×10^4) were exposed to DS-PLGA (50 nM), CuCl$_2$ (1 μM), DS-PLGA (50 nM) plus CuCl2 (1 μM), 5-FU (200 μM) or sorafenib (20 μM) for 6 h. The cells were collected and sub-cultured in 6-well plates containing drug-free medium at a cell density of 2.5×10^3/well. After 10 days culture, the clonogenic cells were determined by counting the colonies containing at least 50 cells.

In vitro HCC sphere cell culture

To culture the HCC spheres, cells were cultured in poly-HEMA coated ultra-low adherence flasks or plates to prevent cell adhesion. The spheres were cultured, at a density of
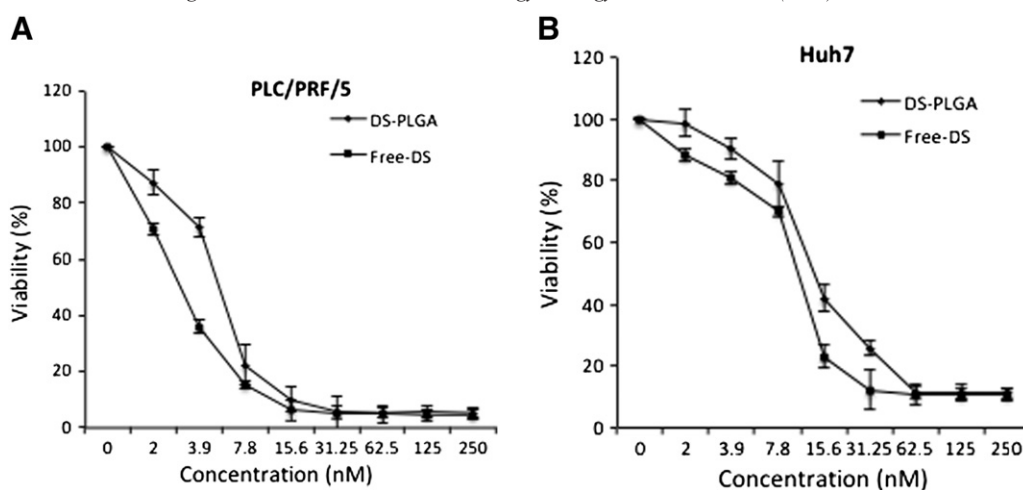
Figure 2. *In vitro* cytotoxicity of DS-PLGA in HCC cell lines. The PLC/PRF/5 **(A)** and Huh7 **(B)** HCC cell lines were exposed to drugs for 72 h and subjected to typical MTT cytotoxicity assay. n = 3, the vertical bars represent SD. **(C)** PLC/PRF/5 and Huh7 cell lines were subjected to different treatments for 4 h. The DNA contents were measured by flow cytometry analysis. Typical histograms are presented. n = 3; $**P < 0.01$.

5000 cells/ml, in stem cell culture medium [SCM, serum-free DMEM-F12 supplemented with B27 (Invitrogen, Paisley, UK), 20 ng/ml epidermal growth factor (EGF, Sigma), 10 ng/ml basic fibroblast growth factor (b-FGF, R & D System, Abingdon, UK)]. After 7 days of culture, the spheres were subjected to different treatments.

In vitro migration and invasion assay

Cell invasion and migration assays were performed using cell culture inserts (Millipore) coated with or without Matrigel (BD Bioscience, Bedford, MA, USA), respectively. Cells (5×10^4) were resuspended in 200 μl serum-free DMEM and placed in upper chamber of the insert. The lower chamber was filled with medium containing 10% FCS. After 48 h incubation at 37 °C, migrated cells were fixed by methanol and stained in 0.5% crystal violet. Cells in six random microscopic fields were counted.

HCC xenograft and in vivo metastasis experiments

Five-week-old female BALB/c Nu/Nu athymic nude mice (Biotechnology & Cell Biology Shanghai, China) were housed under pathogen-free conditions according to the Third Military Medical University (TMMU) animal care guidelines and the animal experiments were reviewed and approved by the Ethical Committee of TMMU. PLC/PRF/5 cells (5×10^5) were subcutaneously injected at one front flank of the mice. When the tumor volume (V) reached ~200 mm³, the tumor bearing mice were randomly subdivided into 8 groups (8 mice/group): 1. Control: no treatment; 2. Copper gluconate (CuGlu) 6 mg/kg p.o.; 3. Empty PLGA i.v.; 4. Free DS 10 mg/kg p.o. + CuGlu 6 mg/kg p.o.; 5. DS-PLGA 2.5 mg/kg i.v. + CuGlu 6 mg/kg p.o.; 6. DS-PLGA 5 mg/kg i.v. + CuGlu 6 mg/kg p.o.; 7. DS-PLGA 10 mg/kg i.v. + CuGlu 6 mg/kg p.o.; 8. DS-Lipo 10 mg/kg i.v. + CuGlu 6 mg/kg p.o. We chose copper gluconate for *in vivo* study because it showed similar effect *in vitro* (Table 2) and is more tolerable by animal. The animals were treated 3 times/week for successive 3 weeks. The xenograft size

was recorded trice per week. The tumor volume was calculated by the following formula: V = (L × W²) × 0.5, where L is the length and W is the width of the tumor. After 3 weeks, the animals were sacrificed. The tumors were removed, photographed and subjected to further analysis.

The *in vivo* lung metastasis mouse model was established by injecting 5×10^6 single-cell suspension of PLC/PRF/5 cells (in 200 μl of PBS) into the tail vein. After 2 weeks, the mice were treated 3 times/week with 10 mg/kg DS-PLGA i.v. and CuGlu 6 mg/kg p.o. for 4 successive weeks. The mice were sacrificed two days after the last treatment. The lungs were removed and formalin-fixed for paraffin embedment and H&E staining.

Immunohistochemistry and H&E staining

The sections from paraffin embedded tumor and normal tissues were stained with primary antibodies (Ki-67, 1:200; BAX, 1:200; NFkBp65, 1:200; ALDH1, 1:200) then biotinylated secondary antibody and followed by incubation in ABC reagent (Dako Labs, Cambridgeshire, UK). For H&E staining, the paraffin-embedded sample slides were stained with hematoxylin and eosin and the slides were mounted with coverslips using Permount (Fisher Sci, Loughborough, UK).

Statistical analysis

The statistical significance of treatment outcomes was assessed using the Student's *t*test and one-way ANOVA; $P < 0.05$ was considered statistically significant in all analyses.

Results

Physicochemical characterization of DS loaded PLGA nanoparticles

The influence of PLGA:DS ratio and sonication/homogenizing time on the EE, DLC and nanoparticle size were examined. The PLGA:DS ratio of 2:1 (w/w) and 4 min of sonication
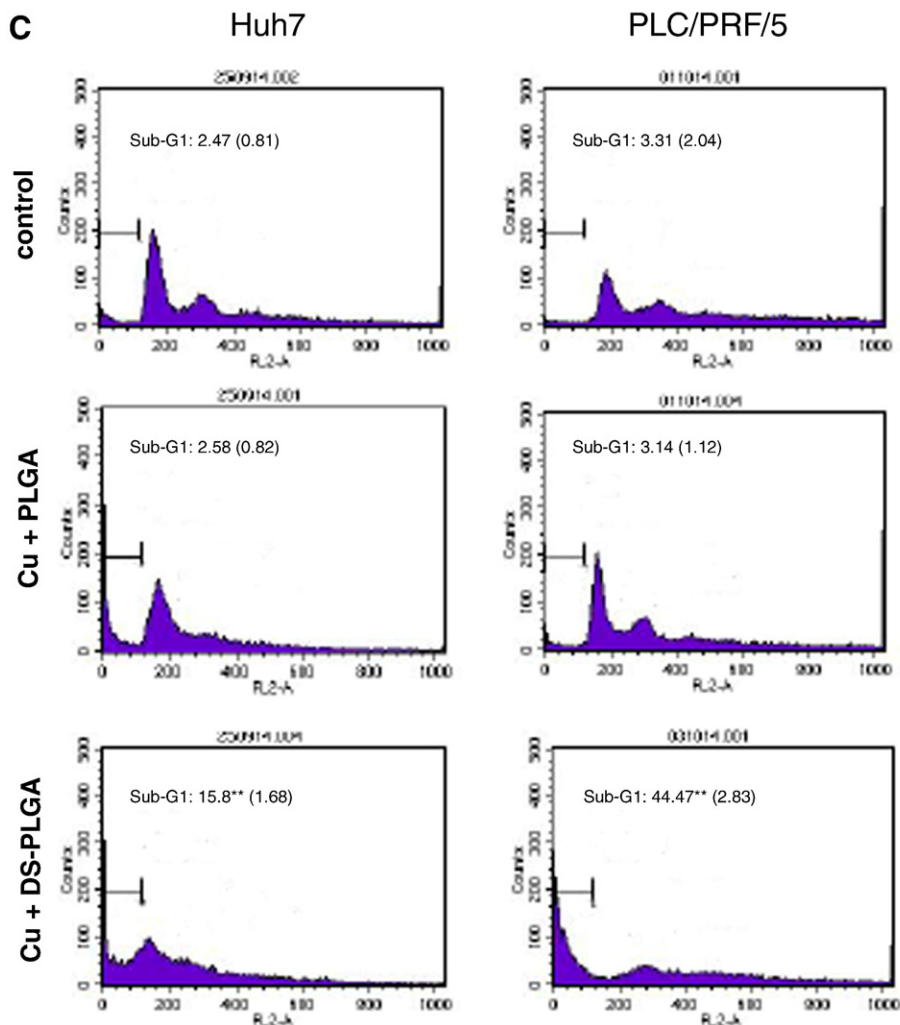
Figure 2 *(continued)*.

provided us with the most optimum nano-characteristics with most narrow size (131.8 ± 6.9 and 136.2 ± 6.2 nm) and satisfactory zeta potential (−22.3 ± 0.8 and −21.7 ± 0.96 mV) distribution between the empty and DS loaded PLGA nanoparticles (Table 1 and Supplementary Tables S1 and S2). The SEM image showed that the DS-PLGA was in analogous spherical shapes (Figure 1, B). DS-PLGA showed high EE (78.92 ± 2.16%) with satisfactory DLC (27.67 ± 3.47%).

To determine the stability and release of DS in DS-PLGA, the DS-PLGA was incubated in 1%, 5% and 10% BSA solutions at 37 °C. The particle size was increased in a time and BSA concentration-dependent manner (Figure 1, C). The zeta potential of the DS-PLGA was also examined after 24 h incubation in

BSA solution. At a physiological concentration of BSA (5%), the DS-PLGA maintained a satisfactory particle size (162 nm) and zeta potential (−15.8 mV) for at least 8 and 24 h, respectively (Figure 1, D). The DS-PLGA showed very good dispersibility.

In vitro cumulative release and half-life of DS in serum

The cumulative drug release was performed over a period of 7 days in a 0.5% Tween 80 PBS solution (pH 7.4) at 37 °C. The DS concentrations at different time lengths were examined. Results demonstrate a very steady and sustained release of DS over 7 days. Around 20% of DS was released within 24 h and reached a 40% release at day 4, which was maintained until day 7
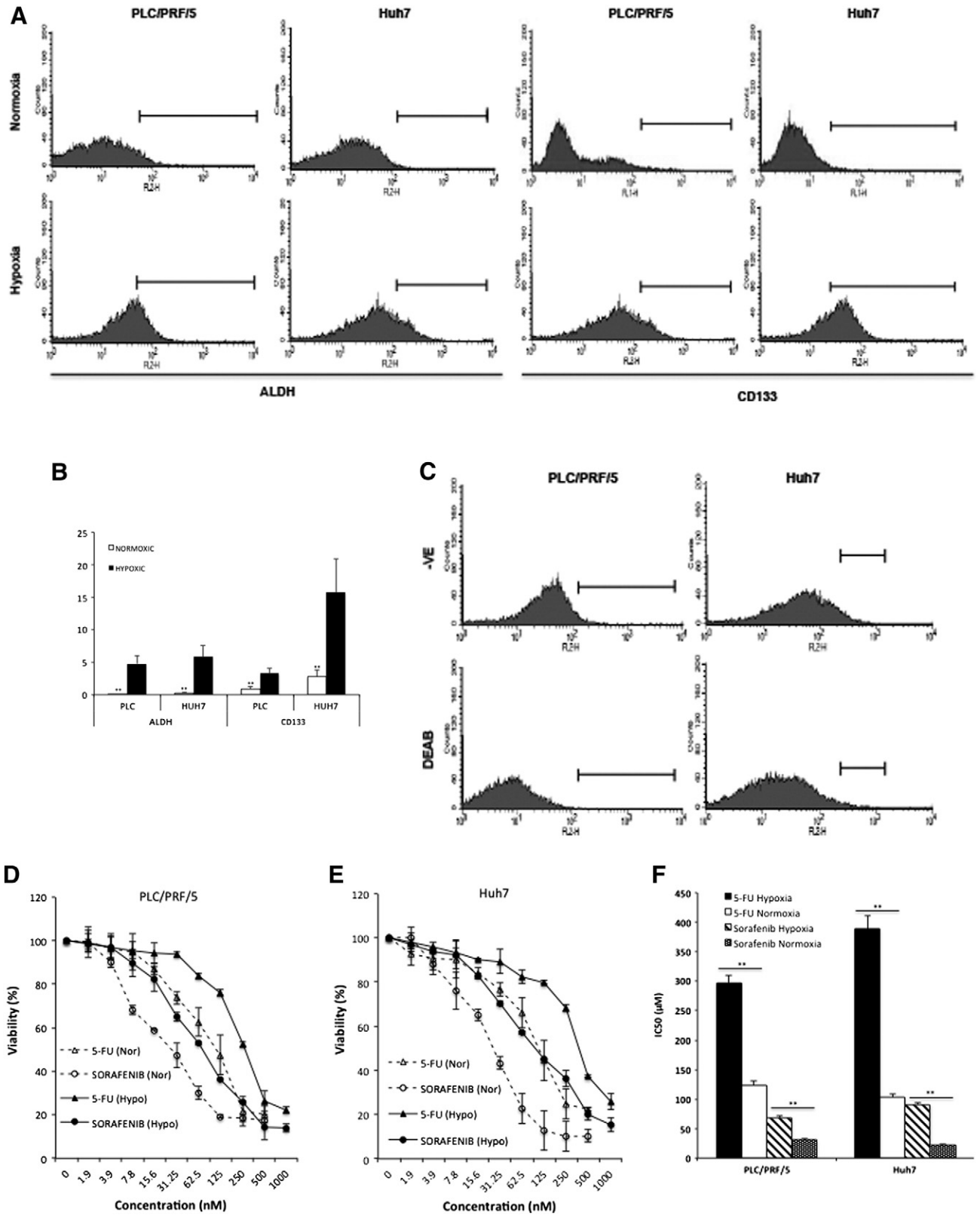
Figure 3. Hypoxia induced expression of CSC marker and chemoresistance in HCC cells. **(A)** and **(B)** PLC/PRF/5 and Huh7 cells were cultured in either normoxic or hypoxic condition for 5 days. The ALDH activity and expression of CD133 were examined by flow cytometry. **(C)** The specificity of ALDH detection was confirmed by DEAB inhibition. **(D–F)** After 72 h exposure, the cytotoxicity of 5-FU and sorafenib was determined in HCC cell lines cultured at normoxic and hypoxic conditions. **$P < 0.01$.
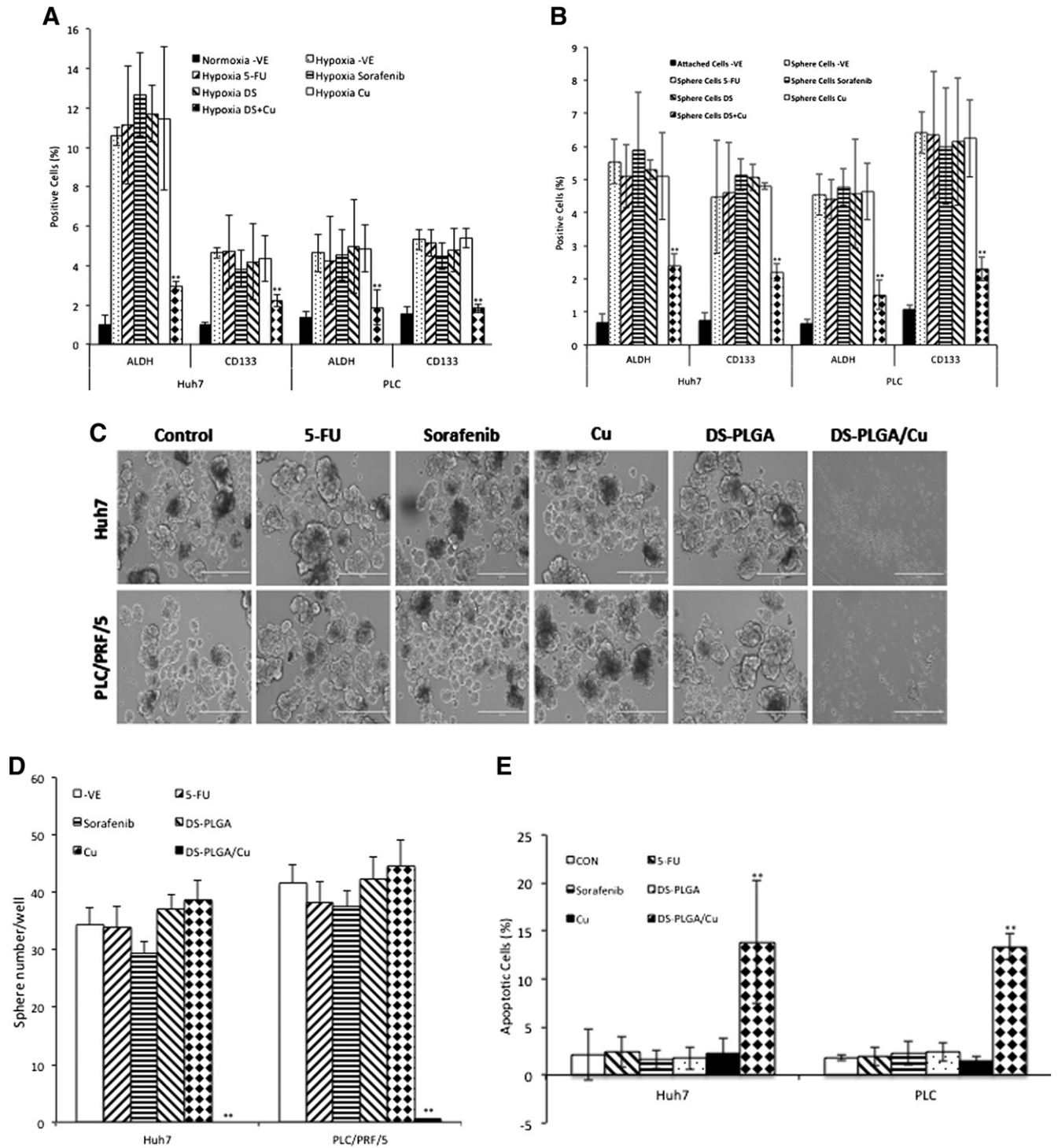
Figure 4. DS-PLGA inhibited hypoxia-induced CSC marker expression, eradicated sphere forming ability and clonogenicity in HCC cell lines. **(A)** Percentage of ALDH and CD133 positive cells. The HCC cells were cultured at hypoxic condition for 5 days and subjected to different treatments for 4 h (DS represents DS-PLGA). **(B)** After exposure of sphere cells to different drugs for 24 h, the ALDH and CD133 positive population was examined by flow cytometry (DS represents DS-PLGA). **(C)** and **(D)** DS-PLGA/Cu blocked the sphere-forming ability in HCC cell. **(E)** and **(F)** DS-PLGA/Cu induced apoptosis in sphere cells. **(G)** and **(H)** DS-PLGA/Cu eradicated clonogenicity in HCC cell lines. n = 3; **P < 0.01.

(Figure 1, *E*). To determine the half-life of DS *in vitro*, the free DS and DS-PLGA (100 μg/ml) were dispersed into horse serum at 37 °C. The free DS was rapidly degraded to undetectable

levels within 30 seconds (Figure 1, *F*). In contrast, DS commenced its release from PLGA at 2 min, equivalent to 34.23 ± 3.38% of the initial drug loading and peaked in 4 min at

Figure 4 *(continued)*.

51.27 ± 5.98%. The controlled release was last for at least 24 h. The half-life of DS-PLGA in serum (7 h) is significantly longer than that of free DS (Figure 1, *G*).
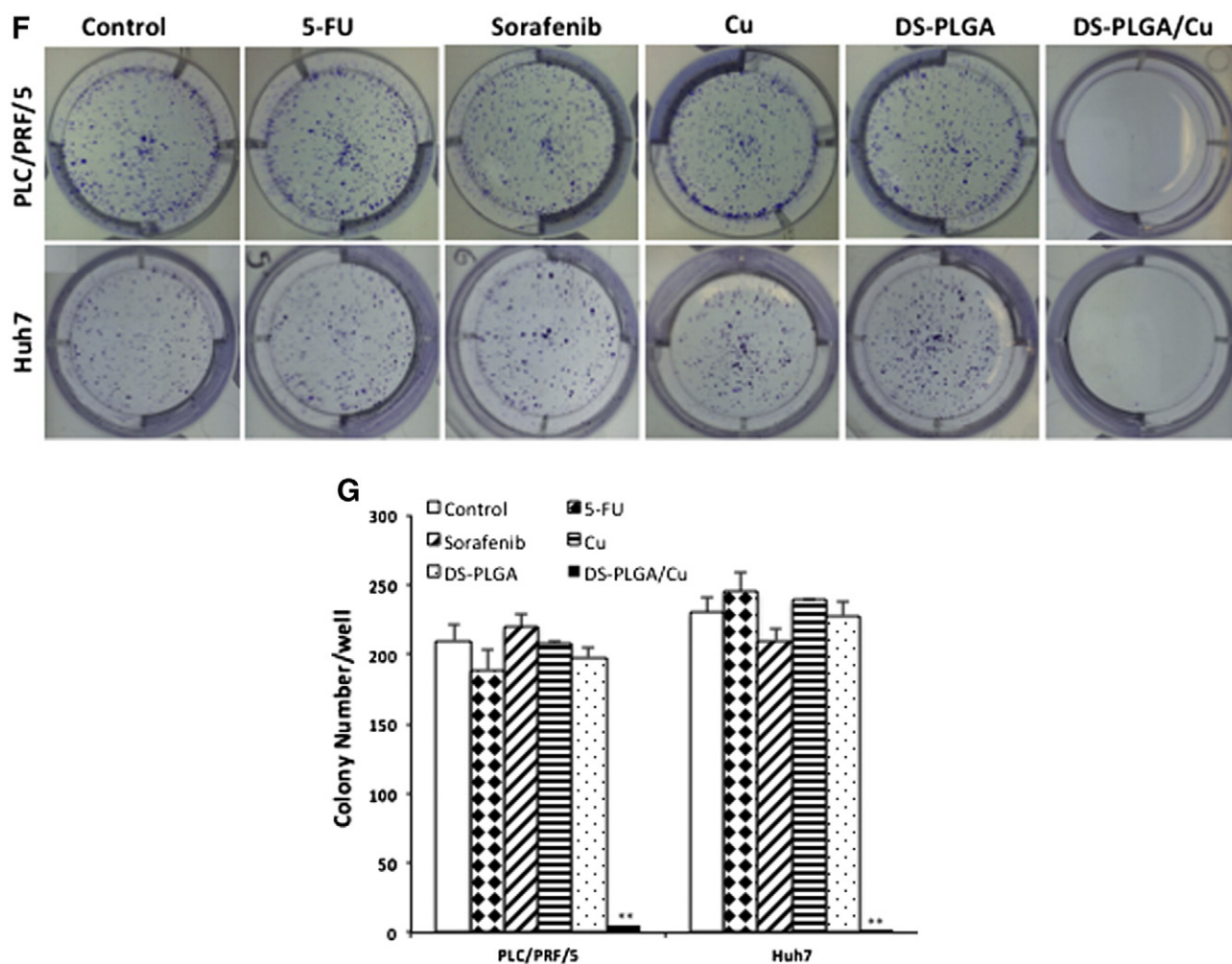
In vitro cytotoxicity of DS-PLGA NPs in HCC cells

The cytotoxicity of DS-PLGA and free DS in PLC/PRF/5 and Huh7 HCC cell lines was compared by MTT assay. $CuCl_2$ (1 μM) was supplemented in all the experiments. The *in vitro* cytotoxicity of DS-PLGA is slightly lower than that of the free DS but no significant difference between the IC_{50s} of DS-PLGA (Huh7, 30.69 ± 3.83 nM; PLC/PRF/5, 49.33 ± 4.11 nM) and free DS (Huh7, 25.34 ± 3.21; PLC, 45.25 ± 3.52 nM) ($P > 0.05$) (Figure 2, *A* and *B*). After exposure to DS-PLGA (50 nM) and $CuCl_2$ (1 μM) for 4 h, the apoptotic cells (sub-G1 population) were identified by DNA content assay using flow cytometry analysis. Background levels of spontaneous apoptotic cells were detected in untreated (2.47% and 3.31%) and PLGA empty nanoparticles plus $CuCl_2$ treated (2.58% and 3.14%) Huh7 and PLC/PRF/5 cell lines respectively. In contrast, massive apoptotic cells (15.68% and 44.47%) were detected in DS-PLGA/$CuCl_2$ treated Huh7 and PLC/PRF/5 cell lines, respectively (Figure 2, *C*).

Hypoxia induced CSC traits and resistance to conventional anticancer drugs

To determine the effect of hypoxia on CSC population, two CSC markers, ALDH and CD133, were examined in hypoxia and normoxia cultured HCC cell lines. The enhanced ALDH activity and elevated expression of CD133 indicated that the CSC population in PLC/PRF/5 and Huh7 cell lines was significantly enlarged by hypoxic environment (Figure 3, *A* and *B*). The specificity of ALDH detection was confirmed by DEAB inhibition (Figure 3, *C*). Furthermore, we examined the chemosensitivity of HCC cell lines at hypoxic condition. When cultured at 1% O_2, the HCC cell lines were significantly resistant to 5-FU and sorafenib (Figure 3, *D-F*).

DS-PLGA inhibited hypoxia-induced CSCs and synergistically enhanced cytotoxicity of 5-FU and sorafenib

Incubation of HCC cells with DS-PLGA (20 nM) and $CuCl_2$ (1 μM) for 24 h significantly reduced the $ALDH^+$ and $CD133^+$ cell population in PLC/PRF/5 and Huh7 cell lines suggesting the sufficient inhibitory effect of DS-PLGA on hypoxia-induced CSCs. In contrast, 5-FU (200 μM), sorafenib (20 μM), Cu or

Table 2
Cytotoxicity of 5-FU, sorafenib, DS-PLGA, 5-FU/DS-PLGA and sorafenib/DS-PLGA in HCC cell lines.

		Huh7	PLC/PRF/5
IC$_{50}$s			
5-FU (μM)		103.26 (6.21)	122.84 (8.14)
Sorafenib (μM)		22.88 (1.26)	30.89 (2.61)
DS-PLGA (nM) + CuCl2		30.69 (3.83)	49.33 (4.11)
DS-PLGA (nM) + CuGlu		38.6 (5.88)	35.5 (7.98)
5-FU (μM)/DS-PLGA (nM) + CuCl2		18.74 (1.09)/18.74 (1.09)	27.56 (1.09)/27.56 (1.09)
Sorafenib (μM)/DS-PLGA (nM) + CuCl2		2.21 (0.19)/22.07 (1.88)	3.08 (0.12)/30.77 (1.17)
CI Values			
	IC50	0.001	0.003
5-FU/DS	IC75	0.001	0.003
	IC90	0.002	0.002
	IC50	0.006	0.051
Sorafenib/DS	IC75	0.010	0.094
	IC90	0.018	0.178

The figures are IC$_{50}$s and CI values, respectively. The numbers in the parentheses are the SD; n = 3. CI values: 0.9-1.1additive effect; 0.8-0.9slight synergism; 0.6-0.8moderate synergism; 0.4-0.6synergism; 0.2-0.4 strong synergism. Both CuCl2 and CuGlu are 1 μM.

DS-PLGA alone had no effect on CSC marker expression (Figure 4, A). Furthermore, the combinational effect of DS-PLGA/Cu and 5-FU or sorafenib was examined using CI-isobologram assay. In combination with DS-PLGA, the in vitro cytotoxicity of 5-FU and sorafenib was significantly enhanced. CI-isobologram analysis indicates very significant synergistic combinational effect among 5-FU, sorafenib and DS-PLGA/Cu in a wide range of IC values (IC$_{50}$ − IC$_{90}$) (Table 2, Figures S1 and S2).

DS-PLGA inhibited expression of CSC markers in spheroid culture and eradicated sphere-forming and clonogenic abilities

CSCs can form spheres in stem cell culture conditions. Sphere-forming ability is widely accepted as a golden standard for in vitro analysis of stemness of CSCs.[27] The effect of different treatments on sphere-forming ability was examined. A significantly higher percentage of ALDH and CD133 positive CSC population was detected in spheroid cells (Figure 4, B). The ALDH and CD133 positive CSC population in the spheres was significantly reduced after exposure to DS-PLGA (20 nM) and Cu (1 μM) for 4 h but not affected by other treatments. The sphere-forming ability was completely abolished after exposure to DS-PLGA (20 nM) plus Cu (1 μM) for 6 h. No inhibiting effect was observed in 5-FU and sorafenib treated cells (Figure 4, C and D). The DS-PLGA/Cu treated HCC CSCs underwent apoptosis (Figure 4, E and F). We next performed clonogenic assay, a traditional method to determine the self-renewal capacity, cancer cell regeneration and CSC traits,[28] to examine the ability of DS-PLGA/Cu to induce the 'reproductive death' in HCC cell lines. The monolayer-cultured PLC/PRF/5 and Huh7 cells were exposed to 5-FU (200 μM), sorafenib (20 μM), CuCl2 (1 μM), DS-PLGA (50 nM) or DS-PLGA (50 nM) plus CuCl2 (1 μM) for 6 h. The treated cells were collected and cultured in 6-well plates containing drug-free medium at a cell density of 500 cells/well for another 10 days. There was no significant difference in colony numbers when the control group was compared with 5-FU, sorafenib and CuCl2 treated groups. In contrast, the colonies in DS-PLGA/ Cu treated group were completely eradicated in both cell lines (Figure 4, G and H).

DS-PLGA blocked migration and invasion ability of hypoxic and sphere-cultured cells in vitro

CSCs have high metastatic ability, another key event responsible for the very poor prognosis of the advanced HCC patients. Because DS-PLGA/Cu shows very strong inhibiting effect on CSC traits in HCC cell lines, we further examined its effect on cell migration and invasion in vitro. The hypoxia (Figure 5, A and B) and CSC (Figure 5, C and D) induced migration and invasion was significantly inhibited by DS-PLGA/ Cu at an extremely low concentration (5 nM) which is only 1/8 to 1/10 of the IC$_{50}$ concentrations for Huh7 and PLC/PRF/5 respectively. At this concentration, no cytotoxicity was observed in both cell lines.

In vivo anti-HCC efficacy of DS-PLGA in mouse xenografts

To assess anti-tumor activity in vivo, 2.5 mg/kg, 5 mg/kg and 10 mg/kg DS-PLGA was intravenously injected into the tail veins of the HCC xenograft bearing mice. In comparison with the control group, 10 mg/kg DS-PLGA significantly inhibited tumor size and tumor weight (Figure 6, A and B). An equivalent oral dose of DS/ Cu or Lipo-DS i.v./oral-Cu, had no effect on the xenografts. This result indicates that the PLGA encapsulation protected DS from degradation in the bloodstream and delivered the intact DS to cancer tissues. DS-PLGA/Cu treatment inhibited the expression of NF-κB p65 and ALDH in the HCC xenografts (Figure 6, C). No significant mouse body weight difference between the control and treated groups and no cytotoxic effect was observed in the vital organs e.g. lung, liver and kidney (Figure 6, D and E).

DS-PLGA and copper blocks HCC lung metastasis in vivo

The very encouraging in vitro anti-migration and invasion data prompted us to examine the anti-metastatic effect of
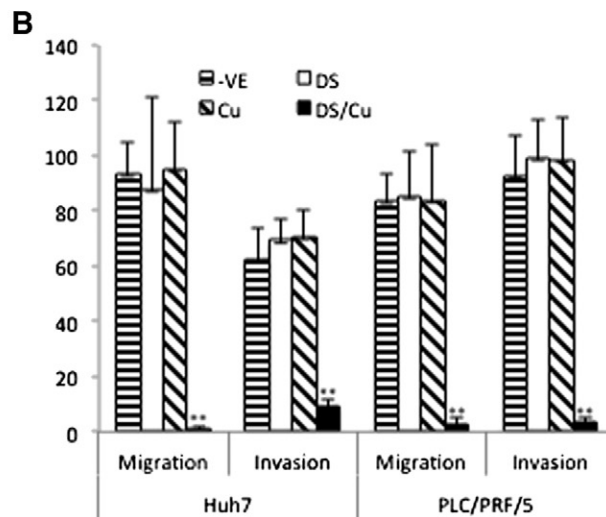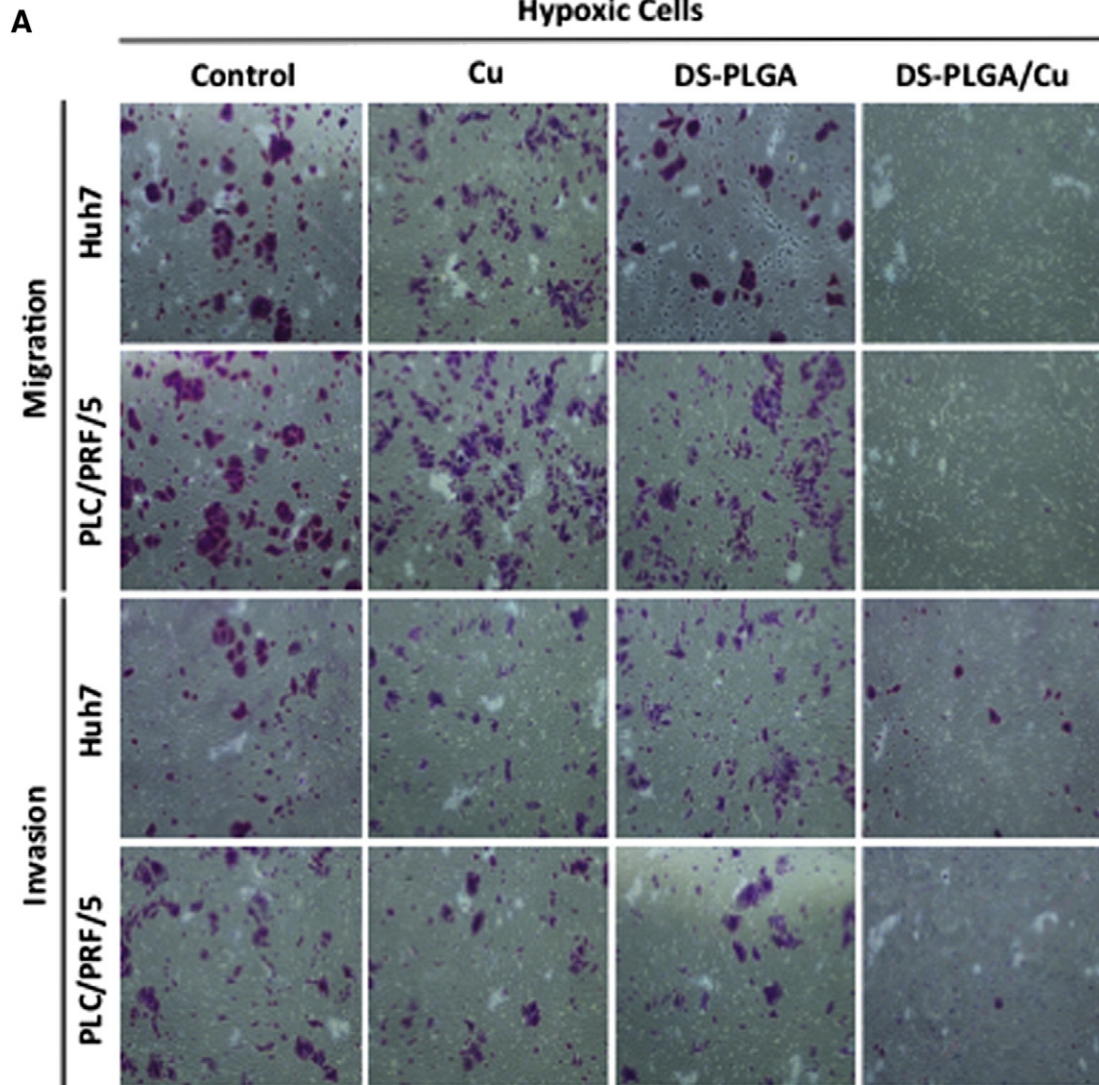
Figure 5. DS-PLGA inhibited migration and invasion ability in hypoxia- and sphere-cultured HCC cells. **(A)** and **(B)** DS-PLGA/Cu inhibited migration and invasion of hypoxic HCC cells. After 7 days hypoxic culture, the HCC cells were subcultured in a transwell containing different chemicals at hypoxic condition for 48 h (DS represents DS-PLGA). **(C)** and **(D)** DS-PLGA/CuCl2 inhibited migration and invasion of HCC CSCs. After 7 days sphere culture, the HCC cells were subcultured in a transwell containing different chemicals at hypoxic condition for 48 h. n = 3; **$P < 0.01$.
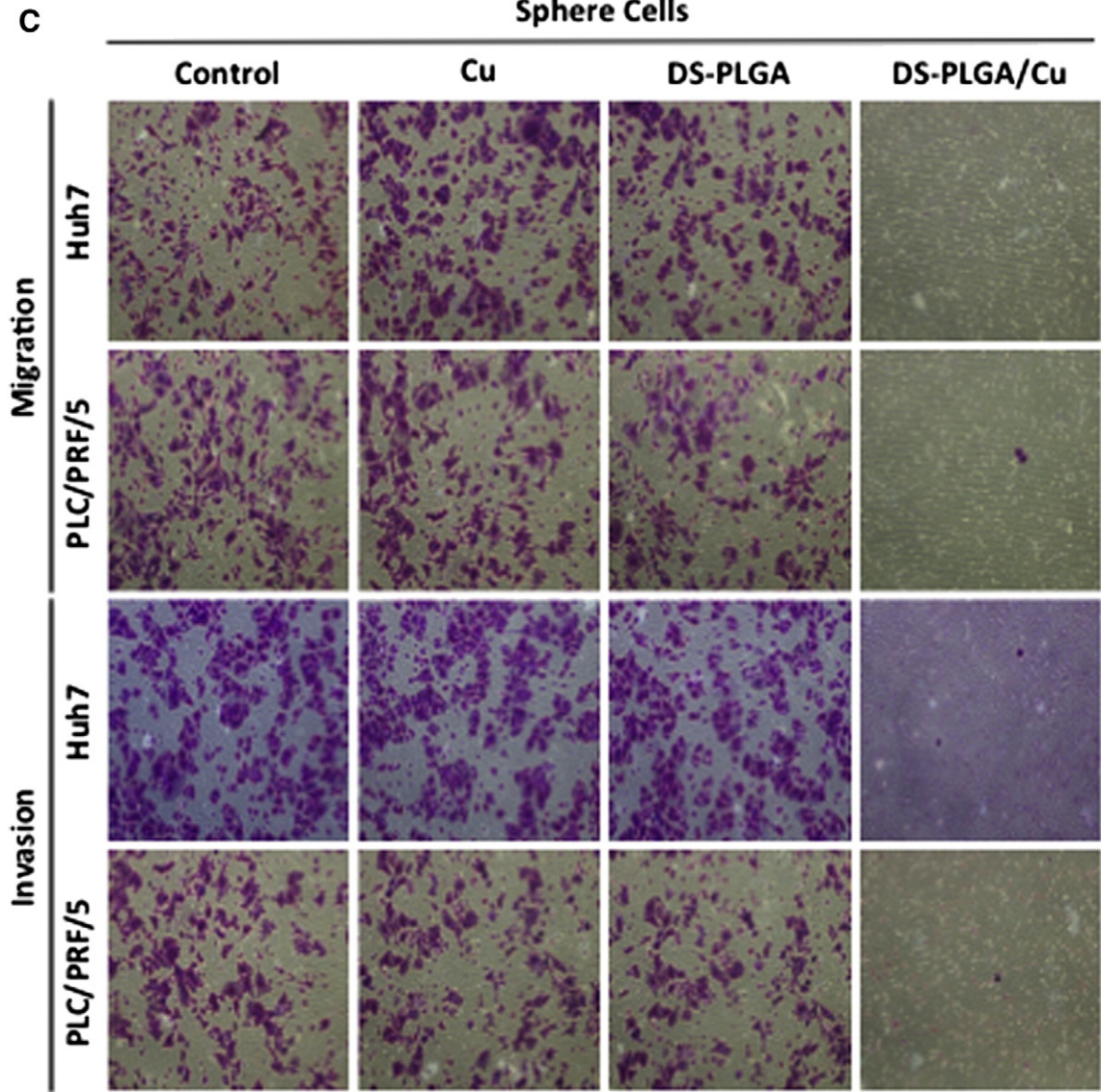
Figure 5 *(continued)*.
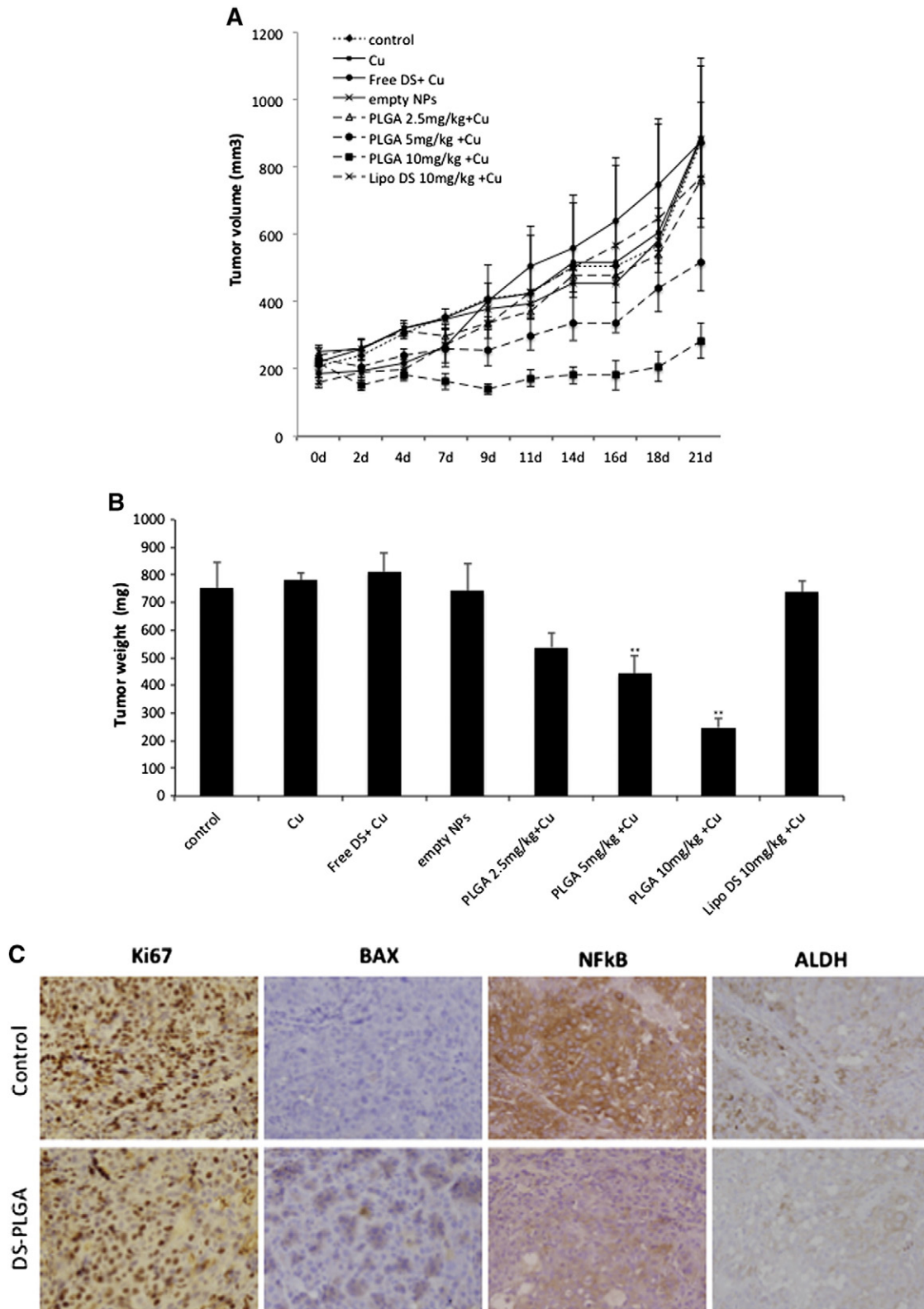
Figure 6. DS-PLGA + Cu inhibited the growth of HCC derived xenografts and the *in vivo* effect on different biological pathways. **(A)** The grow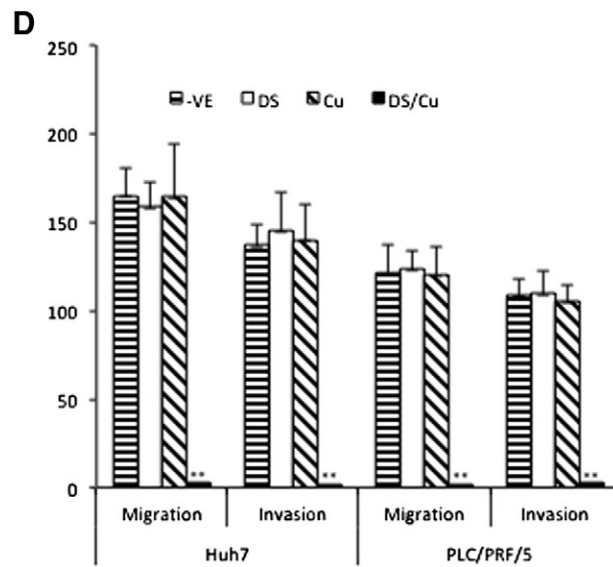th curves of tumor size. The drugs were administered 3 times/week for successive 3 weeks. **(B)** The weight of tumors at the end of experiment. Control: no treatment, Cu: CuGlu p.o., Empty NPs: Empty PLGA i.v., Free DS + Cu: DS p.o. + CuGlu p.o.; PLGA + Cu: DS-PLGA i.v. + CuGlu p.o., Lipo DS + Cu: Liposome DS i.v. + CuGlu p.o. **(C)** The effect of DS-PLGA (10 mg/kg) plus CuGlu (6 mg/kg) on the protein expression of Ki67, BAX, NF-κB and ALDH in HCC xenografts (×400 magnification). **(D)** The body weight changes during the experimental period. **(E)** Representative histopathological images of lung, liver and kidney in DS-PLGA plus CuGlu treated mice (H&E staining, × 400 magnification).

Figure 6 *(continued)*.

DS-PLGA/Cu *in vivo*. The lung metastasis of the tail vein injected HCC cells was completely blocked by combinational application of DS-PLGA and CuGlu (Figure 7). Cancer nodules and micro-metastasis were observed in the control group but not in the treated animals. All the *in vivo* 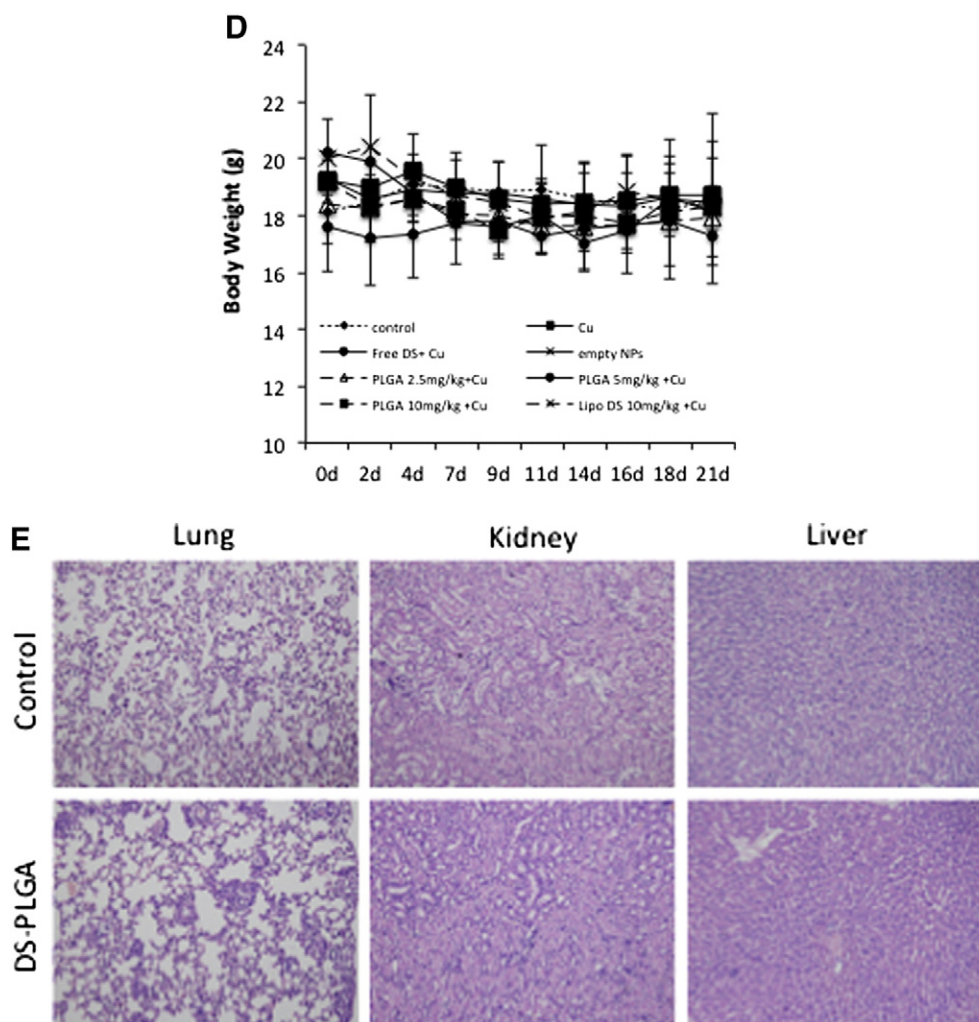experiments were performed with the guidelines approved by the Institutional Animal Care and Use Committee of the Fourth Military Medical University.

Discussion

Only 5-25% of new oncology drugs in clinical development are actually reaching the market.[8,29] This has led to an increasing appreciation of the potential of repurposing known drugs for cancer treatment. DS is highly cytotoxic in several types of cancer cells *in vitro*,[6,10,15,16,30–32] whereas oral administration of free DS does not inhibit tumor growth *in vivo*.[33] Recent publication suggests that the intact sulfhydryl group is essential for the anticancer function of DS.[22,24] The degradation of DS in the bloodstream destroys the sulfhydryl group making DS lose

its cancer targeting ability. The degradation of DS in the serum kinetically results from a covalent interaction of this drug with the free sulfhydryl of serum albumin. The half-life of DS pH 7.4 is 1-1.5 minutes.[19,34,35,36,37] This may introduce the discrepancy between the anticancer activities *in vitro*, *in vivo* and in clinic (ClinicalTrials.gov: NCT00256230, NCT00742911, NCT01118741). Nanomedicine can protect and deliver drugs in the bloodstream.[38] The *in vivo* anticancer efficacy of DS can be improved by liposomal encapsulation (half-life ~25 min).[6,33] In this study, we successfully extended the half-life of DS to ~7 h by encapsulation of DS into PLGA (Figure 1, *G*). We achieved very satisfied EE, DLC, nano-particle size and dispersibility (Table 1). The DS encapsulated nano-particles are stable in physiological concentrations of BSA and the release of DS was steadily controlled at 37 °C. Importantly, after 8 h incubation, the DS concentration in the serum still remained at ~40 μM (12 μg/ml, Figure 1, *F*), which is markedly higher than the IC_{50s} of DS in a wide range of cancer types (~50-500 nM).[6,10,15,16,30–32] DS-PLGA/Cu induced HCC cell apoptosis and the *in vitro* cytotoxicity of DS-PLGA/Cu were comparable to the free DS
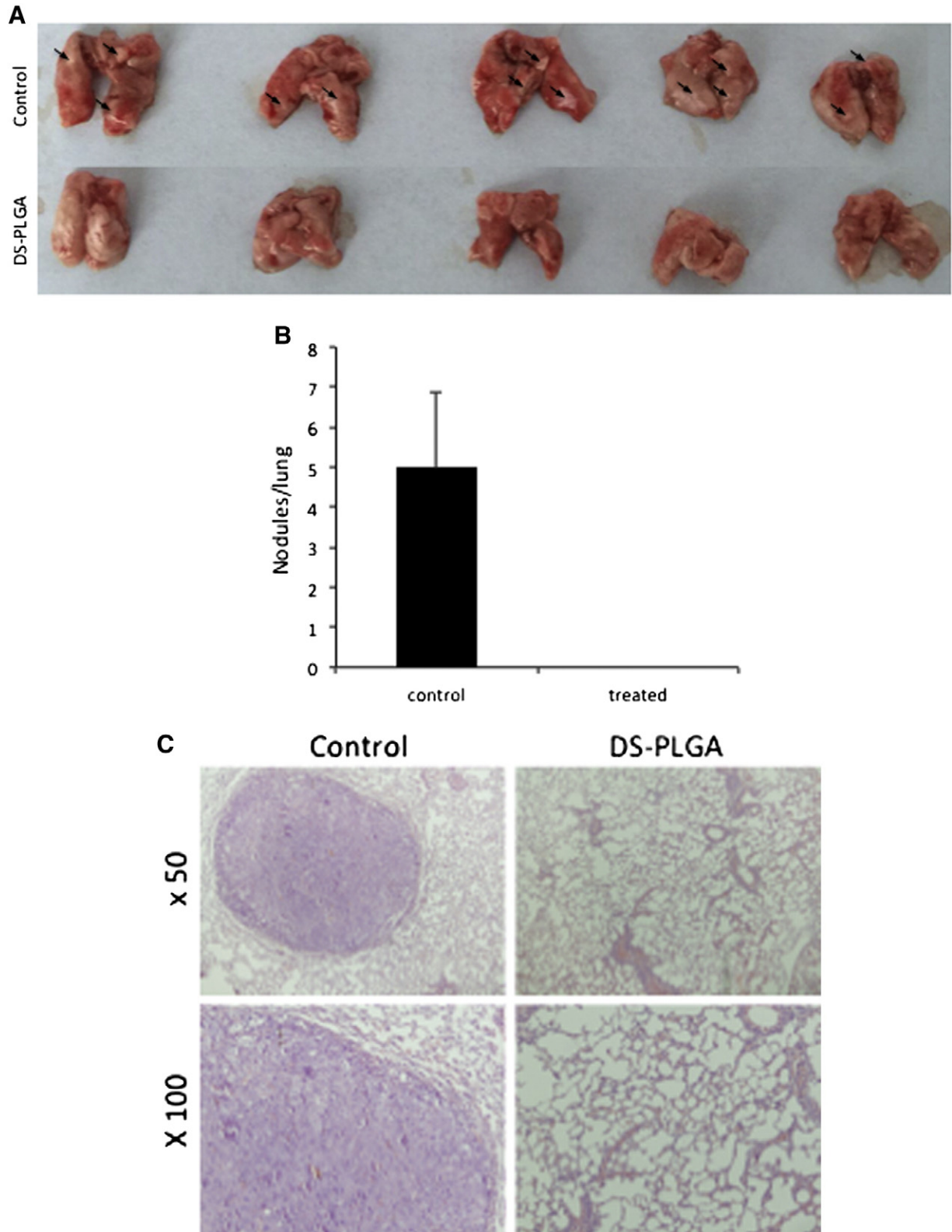
Figure 7. DS-PLGA + CuGlu blocked lung metastasis. **(A)** The images of lung metastatic nodules (black arrows). **(B)** The cancer nodule number in lung. **(C)** Representative H&E staining microscopic images showing the histology of metastatic nodules in mouse lung.

(Figure 2, A and B). Therefore, nanomedicine may be a novel strategy for protection of the sulfhydryl group in DS and translation of DS into cancer treatment.

HCC is resistant to all currently available anticancer drugs with only very marginal response to sorafenib.[4] It has been widely accepted that CSCs display significant resistance to cytotoxic drugs with different resistant mechanisms.[39] Hypoxia is a common feature of HCC. The median partial pressure of O_2 in HCC is 6 mmHg as compared to 30 mmHg in normal liver tissues.[40] Emerging evidence suggests that hypoxia plays pivotal roles in chemoresistance.[41] The hypoxic condition in the stem cell niche is essential for maintaining the stemness in CSCs.[42] Therefore inhibition of hypoxia-induced CSCs may sensitize cancer cells to conventional anticancer drugs. Previous studies indicate that DS targets CSCs and sensitizes several types of cancers to conventional anticancer drugs.[6,10,16,30,32,43,44] Our results demonstrated that hypoxia increased CSC population in HCC cell lines. The hypoxic cells were highly resistant to 5-FU and Sorafenib (Figure 3). DS-PLGA/Cu synergistically enhanced the cytotoxicity of 5-FU and sorafenib in HCC cells (Table 2 and Figures S1 and S2). At a very low concentration (20 nM), DS-PLGA/Cu significantly inhibited the ALDH and CD133 positive CSC population in both hypoxia-induced and spheroid cultured HCC cell lines (Figure 4, A and B). The sphere forming and clonogenic ability in HCC cell lines was completely abolished by very low concentration of DS-PLGA/Cu. In contrast, 5-FU and sorafenib had no effect on CSC population. DS-PLGA/Cu also very strongly in vivo inhibited NF-κB and ALDH activity which are highly responsible for the stemness of CSCs[6,16,30] and efficaciously targeted HCC xenografts at an equivalent to 1/5 of the human antialcoholism dose. The effect of DS-PLGA/Cu on HCC xenografts was dose dependent (Figure 6, A and B). In consistence with our previous study,[6] no toxicity was observed in the vital organs of the DS-PLGA/Cu treated animals (Figure 6, E).

HCC has been shown the hypoxia-induced epithelial-to-mesenchymal transition (EMT), a typical character of CSCs involving in metastasis.[45,46] Liver transplantation is carried out to treat HCC, especially in the early stage. However, due to the extrahepatic organ micrometastasis, the incidence of postoperative recurrence and metastasis is very high (60-100%).[47] Lung remains the most frequent site for HCC metastasis. At the time of diagnosis, most patients have multiple pulmonary or systemic metastasis.[48] There are still no effective systemic therapies available for the metastatic HCC. Therefore development of a drug with anti-metastatic effect will improve HCC treatment.[49,50] DS-PLGA/Cu showed very strong anti-metastatic effect on HCC in vitro (Figure 5) and in vivo (Figure 7), highly in line with our in vivo metastatic lung cancer data (unpublished data). Therefore, DS-PLGA is potentially an effective anti-metastatic drug for HCC treatment.

In conclusion, we showed that the DS-PLGA has very satisfactory EE, DLC, in vitro controlled release and half-life. DS-PLGA and copper showed very strong inhibiting effect on CSCs and synergistic cytotoxicity with 5-FU and sorafenib. It also manifests very promising anticancer efficacy and anti-metastatic activity in HCC mouse model. Our results suggest that nano-controlled delivery system may lead to fast translation of DS into liver cancer treatment.

Appendix A. Supplementary data

Supplementary data to this article can be found online at http://dx.doi.org/10.1016/j.nano.2016.08.001.

References

1. Siegel R, Ma J, Zou Z, Jemal A. Cancer statistics, 2014. Clin 2014;**64**:9-29.
2. Jemal A, Bray F, Center MM, Ferlay J, Ward E, Forman D. Global cancer statistics. Clin 2011;**61**:69-90.
3. Asghar U, Meyer T. Are there opportunities for chemotherapy in the treatment of hepatocellular cancer? J Hepatol 2012;**56**:686-95.
4. Kane RC, Farrell AT, Madabushi R, Booth B, Chattopadhyay S, Sridhara R, et al. Sorafenib for the treatment of unresectable hepatocellular carcinoma. Oncologist 2009;**14**:95-100.
5. Kitisin K, Shetty K, Mishra L, Johnson LB. Hepatocellular stem cells. Cancer Biomark 2007;**3**:251-62.
6. Liu P, Wang Z, Brown S, Kannappan V, Tawari PE, Jiang J, et al. Liposome encapsulated disulfiram inhibits NFκB pathway and targets breast cancer stem cells in vitro and in vivo. Oncotarget 2014;**5**:7471-85.
7. Yamashita T, Wang XW. Cancer stem cells in the development of liver cancer. J Clin Invest 2013;**123**:1911-8.
8. Ashburn TT, Thor KB. Drug repositioning: identifying and developing new uses for existing drugs. Nat Rev Drug Discov 2004;**3**:673-83.
9. Schreck R, Meier B, Mannel DN, Droge W, Baeuerle PA. Dithiocarbamates as potent inhibitors of nuclear factor kappa B activation in intact cells. J Exp Med 1992;**175**:1181-94.
10. Yip NC, Fombon IS, Liu P, Brown S, Kannappan V, Armesilla AL, et al. Disulfiram modulated ROS-MAPK and NFkB pathways and targeted breast cancer cells with cancer stem cell like properties. Cancer 2011;**104**:1564-74.
11. Chen D, Cui QC, Yang H, Dou QP. Disulfiram, a clinically used anti-alcoholism drug and copper-binding agent, induces apoptotic cell death in breast cancer cultures and xenografts via inhibition of the proteasome activity. Cancer Res 2006;**66**:10425-33.
12. Kast RE, Boockvar JA, Bruning A, Cappello F, Chang WW, Cvek B, et al. A conceptually new treatment approach for relapsed glioblastoma: coordinated undermining of survival paths with nine repurposed drugs (CUSP9) by the international initiative for accelerated improvement of glioblastoma care. Oncotarget 2013;**4**:502-30.
13. Hothi P, Martins TJ, Chen LP, Deleyrolle L, Yoon JG, Reynolds B, et al. High-throughput chemical screens identify disulfiram as an inhibitor of human glioblastoma stem cells. Oncotarget 2012;**3**:1124-36.
14. Wang W, McLeod HL, Cassidy J. Disulfiram-mediated inhibition of NF-kappaB activity enhances cytotoxicity of 5-fluorouracil in human colorectal cancer cell lines. Cancer 2003;**104**:504-11.
15. Guo X, Xu B, Pandey S, Goessl E, Brown J, Armesilla AL, et al. Disulfiram/copper complex inhibiting NFkappaB activity and potentiating cytotoxic effect of gemcitabine on colon and breast cancer cell lines. Cancer Lett 2010;**291**:104-13.
16. Liu P, Brown S, Goktug T, Channathodiyil P, Kannappan V, Hugnot JP, et al. Cytotoxic effect of disulfiram/copper on human glioblastoma cell lines and ALDH-positive cancer-stem-like cells. Cancer 2012;**107**:1488-97.
17. Estey T, Piatigorsky J, Lassen N, Vasiliou V. ALDH3A1: a corneal crystallin with diverse functions. Exp Eye Res 2007;**84**:3-12.

18. Ginestier C, Hur MH, Charafe-Jauffret E, Monville F, Dutcher J, Brown M, et al. ALDH1 is a marker of normal and malignant human mammary stem cells and a predictor of poor clinical outcome. *Cell Stem Cell* 2007;**1**:555-67.

19. Agarwal RP, McPherson RA, Phillips M. Rapid degradation of disulfiram by serum albumin. *Res Commun Chem Pathol Pharmacol* 1983;**42**:293-310.

20. Cen D, Brayton D, Shahandeh B, Meyskens Jr FL, Farmer PJ. Disulfiram facilitates intracellular Cu uptake and induces apoptosis in human melanoma cells. *J Med Chem* 2004;**47**:6914-20.

21. Brar SS, Grigg C, Wilson KS, Holder Jr WD, Dreau D, Austin C, et al. Disulfiram inhibits activating transcription factor/cyclic AMP-responsive element binding protein and human melanoma growth in a metal-dependent manner in vitro, in mice and in a patient with metastatic disease. *Mol Cancer Ther* 2004;**3**:1049-60.

22. Tawari PE, Wang Z, Najlah M, Tsang CW, Kannappan V, Liu P, McConville C, He B, Armesilla AL, Wang W. The cytotoxic mechanisms of disulfiram and copper(II) in cancer cells. *Toxicol Res* 2015;**4**:1439-42.

23. D'Autreaux B, Toledano MB. ROS as signalling molecules: mechanisms that generate specificity in ROS homeostasis. *Nat Rev Mol Cell Biol* 2007;**8**:813-24.

24. Lewis DJ, Deshmukh P, Tedstone AA, Tuna F, O'Brien P. On the interaction of copper(II) with disulfiram. *Chem Commun* 2014;**50**:13334-7.

25. Johansson B. A review of the pharmacokinetics and pharmacodynamics of disulfiram and its metabolites. *Acta Psychiatr Scand Suppl* 1992;**369**:15-26.

26. Chou TC, Talalay P. Quantitative analysis of dose-effect relationships: the combined effects of multiple drugs or enzyme inhibitors. *Adv Enzyme Regul* 1984;**22**:27-55.

27. Singec I, Knoth R, Meyer RP, Maciaczyk J, Volk B, Nikkhah G, et al. Defining the actual sensitivity and specificity of the neurosphere assay in stem cell biology. *Nat Methods* 2006;**3**:801-6.

28. Franken NA, Rodermond HM, Stap J, Haveman J, van Bree C. Clonogenic assay of cells in vitro. *Nat Protoc* 2006;**1**:2315-9.

29. Walker I, Newell H. Do molecularly targeted agents in oncology have reduced attrition rates? *Nat Rev Drug Discov* 2009;**8**:15-6.

30. Liu P, Kumar IS, Brown S, Kannappan V, Tawari PE, Tang JZ, et al. Disulfiram targets cancer stem-like cells and reverses resistance and cross-resistance in acquired paclitaxel-resistant triple-negative breast cancer cells. *Cancer* 2013.

31. Safi R, Nelson ER, Chitneni SK, Franz KJ, George DJ, Zalutsky MR, et al. Copper signaling axis as a target for prostate cancer therapeutics. *Cancer Res* 2014;**74**:5819-31.

32. Duan L, Shen H, Zhao G, Yang R, Cai X, Zhang L, et al. Inhibitory effect of disulfiram/copper complex on non-small cell lung cancer cells. *Biochem Biophys Res Commun* 2014;**446**:1010-6.

33. Wang W. *Disulfiram formulation and uses thereof. International Application Published under the Patent Cooperation Treaty (PCT) WO2012/076897 A1*; 2012.

34. Agarwal RP, Phillips M, McPherson RA, Hensley P. Serum albumin and the metabolism of disulfiram. *Biochem Pharmacol* 1986;**35**:3341-7.

35. Gessner T, Jakubowski M. Diethyldithiocarbamic acid methyl ester. A metabolite of disulfiram. *Biochem Pharmacol* 1972;**21**:219-30.

36. Kaslander J. Formation of an S-glucuronide from tetraethylthiuram disulfide (Antabuse) in man. *Biochim Biophys Acta* 1963;**71**:730-1.

37. Prickett CS, Johnston CD. The in vivo production of carbon disulfide from tetraethylthiuramdisulfide (antabuse). *Biochim Biophys Acta* 1953;**12**:542-6.

38. Zhang XQ, Xu X, Bertrand N, Pridgen E, Swami A, Farokhzad OC. Interactions of nanomaterials and biological systems: implications to personalized nanomedicine. *Adv Drug Deliv Rev* 2012;**64**:1363-84.

39. Clevers H. The cancer stem cell: premises, promises and challenges. *Nat Med* 2011;**17**:313-9.

40. Vaupel P, Hockel M, Mayer A. Detection and characterization of tumor hypoxia using pO2 histography. *Antioxid Redox Signal* 2007;**9**:1221-35.

41. Simsek T, Kocabas F, Zheng J, Deberardinis RJ, Mahmoud AI, Olson EN, et al. The distinct metabolic profile of hematopoietic stem cells reflects their location in a hypoxic niche. *Cell Stem Cell* 2010;**7**:380-90.

42. Dean M, Fojo T, Bates S. Tumour stem cells and drug resistance. *Nat Rev* 2005;**5**:275-84.

43. Kast RE, Belda-Iniesta C. Suppressing glioblastoma stem cell function by aldehyde dehydrogenase inhibition with chloramphenicol or disulfiram as a new treatment adjunct: an hypothesis. *Curr Stem Cell Res Ther* 2009;**4**:314-7.

44. Triscott J, Pambid MR, Dunn SE. Bullseye: targeting cancer stem cells to improve the treatment of gliomas by repurposing disulfiram. *Stem Cells* 2015;**33**:1042-6.

45. Wong CC, Kai AK, Ng IO. The impact of hypoxia in hepatocellular carcinoma metastasis. *Front Med* 2014;**8**:33-41.

46. Sampieri K, Fodde R. Cancer stem cells and metastasis. *Semin Cancer Biol* 2012;**22**:187-93.

47. Poon RT, Fan ST, Lo CM, Liu CL, Wong J. Long-term survival and pattern of recurrence after resection of small hepatocellular carcinoma in patients with preserved liver function: implications for a strategy of salvage transplantation. *Ann Surg* 2002;**235**:373-82.

48. Zhang C, Rao J, Tu Z, Ni Y. Surgical resection of resectable thoracic metastatic hepatocellular carcinoma after liver transplantation. *J Thorac Cardiovasc Surg* 2009;**138**:240-1.

49. Llovet JM, Beaugrand M. Hepatocellular carcinoma: present status and future prospects. *J Hepatol* 2003;**38**(Suppl 1):S136-49.

50. Bruix J, Sherman M, Practice Guidelines Committee, American Association for the Study of Liver Diseases. Management of hepatocellular carcinoma. *Hepatology* 2005;**42**:1208-36.